Prehistoric ruptures of the Gurvan Bulag fault, Gobi Altay, Mongolia

Carol S. Prentice,[1] Katherine Kendrick,[2] Kelvin Berryman,[3] A. Bayasgalan,[4] J. F. Ritz,[5] and Joel Q. Spencer[6,7]

Received 17 July 2001; revised 30 March 2002; accepted 8 May 2002; published 3 December 2002.

[1] The 1957 Gobi Altay M8.3 earthquake in southern Mongolia was associated with the simultaneous rupture of several faults, including the Gurvan Bulag reverse fault, which is located about 25 km south of the main strike-slip Bogd fault. Our study of paleoseismic excavations across the Gurvan Bulag fault suggests that the penultimate surface rupture occurred after 6.0 ka, most likely between 2.6 and 4.4 ka, and a possible earlier rupture occurred after 7.3 ka. Our interpretation of the stratigraphic relations in one of the exposures suggests that at least five earthquakes have generated surface rupture of the Gurvan Bulag fault since the abandonment of an ancient alluvial fan surface. Luminescence dating of sediment associated with this surface indicates that it formed either 26.6 ± 2.1 ka or 16.1 ± 2.0 ka. These data imply that the recurrence intervals for surface faulting on the Gurvan Bulag and Bogd faults are similar, on the order of several thousands of years, but that the penultimate surface ruptures of the two faults did not occur during the same earthquake. *INDEX TERMS:* 7221 Seismology: Paleoseismology; 8107 Tectonophysics: Continental neotectonics; 8010 Structural Geology: Fractures and faults; *KEYWORDS:* paleoseismology, reverse fault, Gobi Altay, Mongolia, luminescence dating

Citation: Prentice, C. S., K. J. Kendrick, K. Berryman, A. Bayasgalan, J. F. Ritz, and J. Q. Spencer, Prehistoric ruptures of the Gurvan Bulag fault, Gobi Altay, Mongolia, *J. Geophys. Res.*, *107*(B12), 2321, doi:10.1029/2001JB000803, 2002.

1. Introduction

[2] The Gobi-Altay earthquake of 4 December 1957, in southern Mongolia, is one of the world's largest recorded intracontinental earthquakes and one of four great earthquakes that have occurred in or near Mongolia this century (Figure 1) [*Baljinnyam et al.*, 1993]. The rupture pattern associated with this M8.3 earthquake is remarkably complex, involving strike-slip and reverse faulting on several distinct geological structures in a zone about 260 km long and 40 km wide (Figure 2) [*Florensov and Solonenko*, 1965; *Bayarsayhan et al.*, 1996; *Kurushin et al.*, 1997]. This study is focused on one of these structures: the Gurvan Bulag fault zone, a 23-km-long reverse-fault rupture on the southern flank of Ih Bogd, the highest peak of the Gobi-Altay mountain range (Figure 3). The Gurvan Bulag fault rupture is subparallel to and about 25 km south of the Bogd fault, which is the main, left-lateral strike-slip fault. Scarps reported as forming during the 1957 earthquake along the Gurvan Bulag zone are up to 5.2 m high [*Kurushin et al.*, 1997].

[3] Immediately after the 1957 earthquake, a team of Russian and Mongolian geologists began studies of the rupture zone [*Florensov and Solonenko*, 1965]. This work was recently revisited and expanded upon by *Baljinnyam et al.* [1993], who studied a number of the active faults in Mongolia, and by *Kurushin et al.* [1997], who conducted detailed field mapping at many sites along the Gobi-Altay ruptures. The Gurvan Bulag ruptures are associated with a set of low hills that occupy a position south of the main mountain mass (Figure 3). These hills are related to uplift and deformation associated with prior ruptures of the Gurvan Bulag fault zone. *Florensov and Solonenko* [1965] used the term "foreberg" to describe these and similar hills associated with thrust and reverse faulting both north and south of the Bogd fault [*Kurushin et al.*, 1997].

[4] One slip-rate site has been studied along the Bogd fault: *Ritz et al.* [1995] estimated a maximum rate of 1.2 mm yr^{-1} based on offset alluvial fans dated using cosmogenic radionuclide techniques. This slip rate suggests recurrence intervals on the order of 5000 years for surface rupture similar to that of 1957 on the Bogd fault. This work has been recently updated incorporating a correction in the production rate of 10Be, giving a revised slip rate of 1.5 ± 0.4 mm yr^{-1}, suggesting recurrence intervals of 3.7 ± 1.3 kyr (J. F. Ritz, personal communication, 2002). A vertical slip rate along the Gurvan Bulag fault of 0.8–1.2 mm yr^{-1} during the Holocene has been estimated by *Ritz et al.* [1999], suggesting an average recurrence interval of 3000–5000 years. No slip rate estimates have been made for any other structures involved in the 1957 rupture.

[1]U.S. Geological Survey, Menlo Park, California, USA.
[2]U.S. Geological Survey, Pasadena, California, USA.
[3]Institute of Geological and Nuclear Sciences Ltd., Lower Hutt, New Zealand.
[4]GeoInformatics Research and Training Center, Mongolian University of Science and Technology (MUST), Ulaanbaatar, Mongolia.
[5]Institut des Sciences de la Terre, de l'Eau et de l'Espace de Montpellier, Universite Montpellier II, Montpellier, France.
[6]Department of Earth Sciences, University of California, Riverside, Riverside, California, USA.
[7]Now at School of Geography and Geosciences, University of Saint Andrews, St. Andrews, Fife, Scotland.

0148-0227/02/2001JB000803$09.00

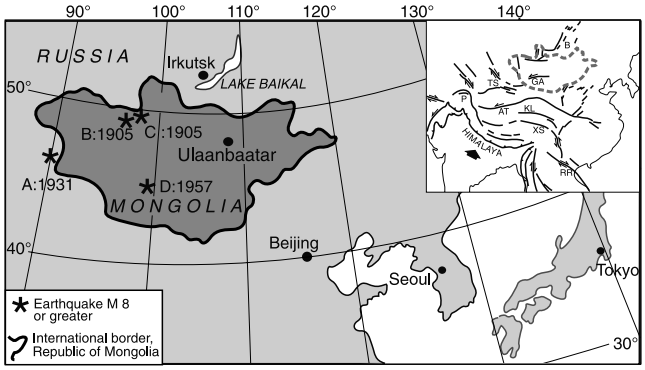

Figure 1. Map showing locations of great 20th-century earthquake epicenters in and near Mongolia. A = M8 Fuyun earthquake; B = M8.2 Bulnay earthquake; C = M8.4 Tsetserleg earthquake; D = M8.3 Gobi Altay earthquake, subject of this study. (Modified from *Baljinnyam et al.* [1993].) Inset shows tectonic setting and major regional faults. RR = Red River fault; XS = Xianshuihe fault; AT = Altan Tagh; KL = Kun Lun; P = Pamir; TS = Tien Shan; GA = Gobi Altay, B = Baikal Rift. Dashed line shows international border of Mongolia.

[5] Our study is aimed at developing an understanding of the nature of prehistoric ruptures of the Gurvan Bulag fault zone. In particular, our goal is to constrain the timing of the penultimate earthquake rupture of the Gurvan Bulag fault zone. Such constraints would allow us to determine whether the penultimate rupture on the Gurvan Bulag may have coincided with the penultimate rupture on the Bogd fault. Whether complex intracontinental events such as the 1957 Gobi Altay earthquake are typical of earthquakes on the Bogd fault, with multiple structures repeatedly rupturing together, or whether the 1957 event is unique in its complexity can only be determined by dating prehistoric events on the individual structures that ruptured in 1957.

[6] We studied five exposures (hand-dug trenches and natural stream cuts) along the main Gurvan Bulag fault zone, and one exposure across a secondary backthrust 0.6 km north of the main fault (Figure 4). All exposures showed stratigraphic evidence of multiple ruptures such as faulted colluvial wedges and/or subsurface fault terminations. We collected samples from all but one of these exposures for luminescence dating (thermoluminescence, TL, and optically stimulated luminescence, OSL) (Tables 1, 2, and 3). Infrared OSL (IR OSL) was performed on feldspars, and green light OSL (GSL) on quartz grains. These, and radiocarbon samples from site 5 (Table 4), provide constraints on the timing of prehistoric earthquakes on the Gurvan Bulag fault. Luminescence analyses were conducted at two laboratories: samples OSL 1, 2, and 3 were analyzed at the Desert Research Institute in Reno, NV (Table 1). The remaining luminescence samples (OSL 4, 6, 8, 9, 10, 12, 13, and 14) were analyzed at the University of California, Riverside (Table 2).

[7] The trenches and stream cuts were excavated into alluvial sediment associated with several distinct geomorphic surfaces. We conducted reconnaissance mapping of these surfaces using 1:25,000-scale aerial photographs in the regions surrounding our excavation sites, collected samples for luminescence and radiocarbon dating from the underlying sediment, and measured profiles of the risers between the surfaces and across the fault scarps that offset them. Our mapping suggests a minimum of three terrace levels: a high fan surface, T3, and two terraces inset into the T3 surface, T2 and T1, that are situated above the modern, active channels (Figure 5).

2. Description and Interpretation of Exposures

[8] We selected four study sites near the western end of the 1957 rupture, where the scarp height is relatively low (2–4 m) and where the fault zone and associated sediment were exposed in several stream cuts. We cleaned and logged natural exposures in two stream cuts (sites 1 and 4) and dug shallow excavations at two sites in between the streams (sites 2 and 3; Figure 4A). We collected samples for luminescence dating at three of these four sites, and a single sample for radiocarbon dating. Of these four sites, three were excavated into the sediment underlying surface T3, and one (site 3) was excavated into sediment underlying surface T2 (Figure 5A). We selected another excavation site (site 5) along the main rupture 3.5 km southeast of site 1, where we found organic-rich sediment exposed near the fault scarp in a stream cut (Figure 4B). This site was excavated into sediment underlying an inset terrace occupying the same geomorphic position as T2 (Figure 5B). Site 6 is located on a secondary structure of the Gurvan Bulag fault zone, a backthrust approximately 0.6 km north of the main fault. The trench at this site was excavated into a surface that was higher and older than the T3 fan surface (Figure 4B).

2.1. Western Sites, 1–4

[9] **Site 1 (Western Creek)** is one of four sites located along a 320-m-long section near the western end of the 1957 rupture (Figure 5). At this site a 2.5-m-high, natural stream-cut provides an exposure of alluvium and colluvial deposits involved in a complex zone of reverse and thrust faults that deform the T3 surface (Figure 6A). We mapped the exposure at a scale of 1:20 (Figure 6B). The light gray (Munsell color 10YR7/2) interbedded sand and gravel alluvial fan deposits north of the fault zone are distinct from the massive, unsorted, yellowish-brown (Munsell color 10YR5/6) colluvial deposits that are preserved south of the fault zone (Figure 6A).

[10] Figure 6B shows the deformation of the alluvial units near and within the fault zone. Beds are folded in a manner consistent with drag on the hanging wall of a reverse fault (for example, units 20–50). We subdivided the colluvial deposits into five distinct units, labeled C1–C5, in the area between faults 3 and 4. We interpret each colluvial unit to represent an individual fault slip event: each time the fault breaks and refreshes the scarp, a new influx of colluvium is deposited on the ground surface above the footwall. This scarp-derived colluvial material typically accumulates in a wedge-shaped deposit known as a colluvial wedge [*McCalpin*, 1996; *Yeats et al.*, 1997].

[11] Faults F1 and F2 break through all of the exposed alluvial units and colluvial packages C2 and C3. Fault F3 breaks colluvial deposits C3–C5. Colluvial units C1 and C1a are not faulted, which is evidence that these deposits postdate the 1957 earthquake. All of the colluvial units

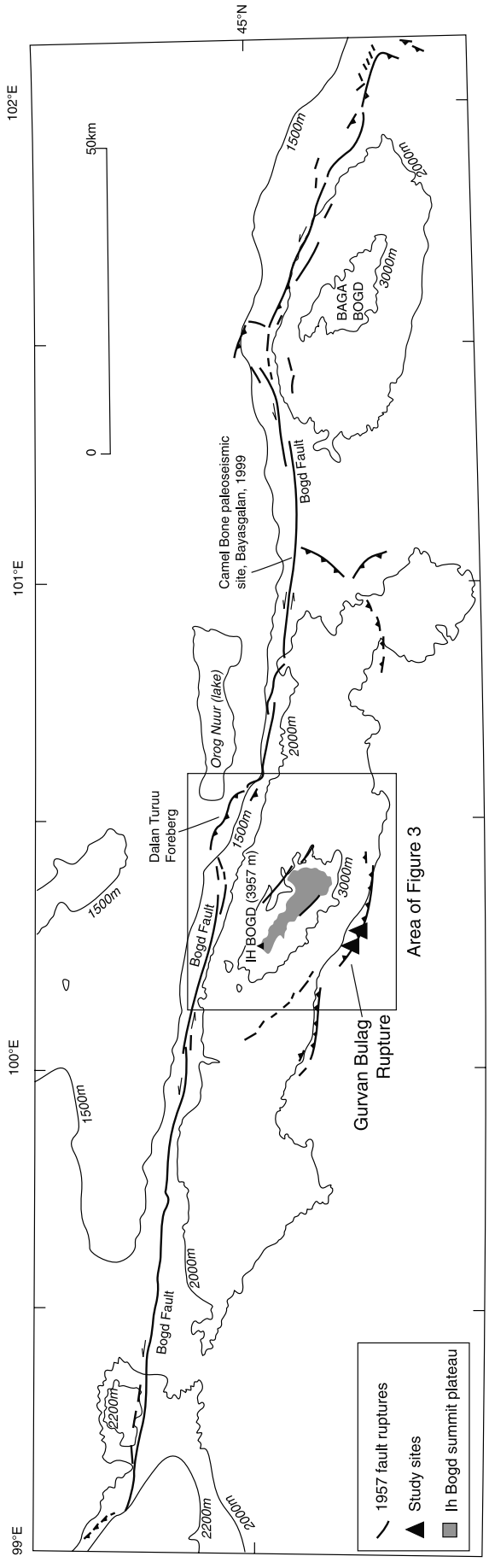

Figure 2. Map showing ruptures associated with 1957 Gobi Altay M 8.3 earthquake, and location of study area. The Gurvan Bulag fault zone, about 25 km south of the main strike-slip Bogd fault, is one of several distinct structures that ruptured during this earthquake. Sites 1–4 are located in the region marked by the western triangle, sites 5–6 by the eastern triangle. (Modified from *Baljinnyam et al.* [1993].)

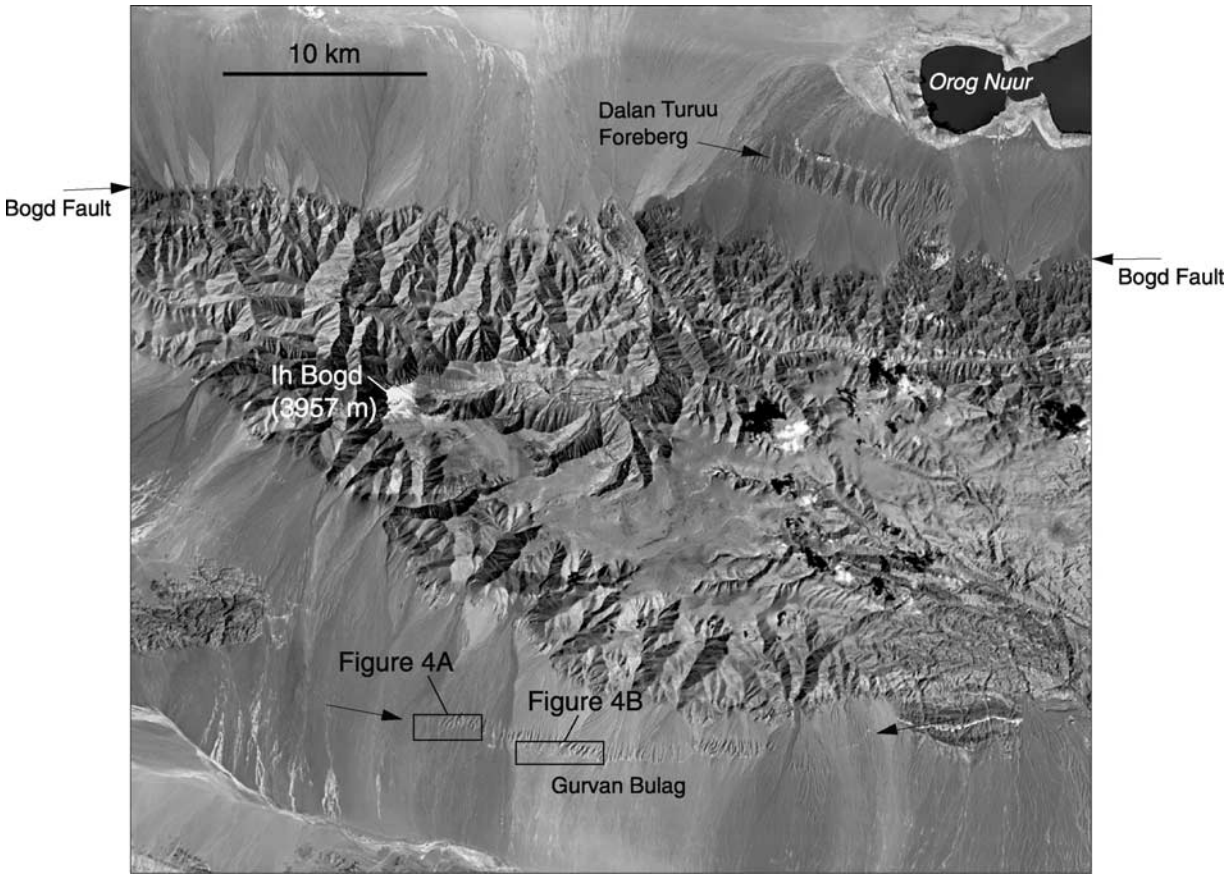

Figure 3. Landsat TM satellite image of Gurvan Bulag and Ih Bogd area. Area shown is part of path 135, row 29; image taken 21 August 1990. Gurvan Bulag region, subject of this study, is shown near bottom of image. Arrows in lower part of image show approximate limits of 1957 Gurvan Bulag ruptures. Rectangles show areas of Figures 4A and 4B. Image processed by M. Rymer, USGS.

older than C1 and C1a are faulted, and must therefore predate the 1957 earthquake. We interpret these older colluvial deposits to represent the sedimentary responses to prehistoric ruptures of this fault zone. Note that faults F1 and F2 extend to the surface, truncating fault F3, indicating that fault F3 was inactive in 1957. Fault F4 was active in 1957; it displaces only one prehistoric colluvial deposit, which we correlate with C2. Fault F5 is a minor backthrust, which offsets unit 10 about 30 cm.

[12] These relations suggest that at least five faulting events, including the 1957 event, have ruptured the alluvial deposits exposed in this stream cut. Because we found no material suitable for radiocarbon or luminescence dating at this site, we have no direct age control. However, all of these events must have occurred after the abandonment of the T3 alluvial fan surface.

[13] The amount of displacement of colluvium C2a provides a minimum estimate of the amount of 1957 dip slip across fault F4. C2a was deposited in response to the penultimate earthquake, and therefore has only been faulted by the 1957 event. The distance along the fault between A and A′, 170 cm, is a minimum amount of 1957 slip on this fault plane. The minimum 1957 dip slip across fault F1 can similarly be estimated by measuring the distance C2 is faulted: approximately 40 cm. Collectively, these measurements suggest a minimum of 2.1 m of 1957 fault slip at this site.

[14] **Site 2 (Double Scarp site)** is a hand-dug trench excavated into the T3 surface about 40 m southeast of site 1 (Figure 5). At this location, two fault zones, 4–6 m apart, ruptured in 1957 (Figure 7). Units 20 and 10 are alluvial fan deposits and an overlying silt cap, respectively, that have been disrupted by both fault zones. Remnants of free faces produced by the 1957 earthquake are present along both of these fault zones at or very near the location of the exposure. Two small colluvial deposits have accumulated since the 1957 earthquake, C1 and C1a. The hatchured area marks the ground surface at the time of the 1957 earthquake. This horizon is vesiculated and darkened by soil-forming processes, and C1 buries part of this former ground surface between meters 4 and 5. Near meter 7, we found dead grass (sample RC1) along this horizon that was overridden by the upper plate of a low-angle 1957 fault (F2). Radiocarbon analysis of this sample yielded an age of 0–320 years B.P. (All radiocarbon dates discussed in text are dendrochronologically calibrated, 2σ age ranges.) and concurs with our interpretation that this surface was overridden in 1957 (Table 4). The distance along fault F2 between the tip of the fault where it is overlain by C1 near meter 5 (point A), and the northernmost point of the old ground surface near meter 7 (point A′), is about 2 m (A to A′). This distance is a minimum 1957 displacement on fault F2.

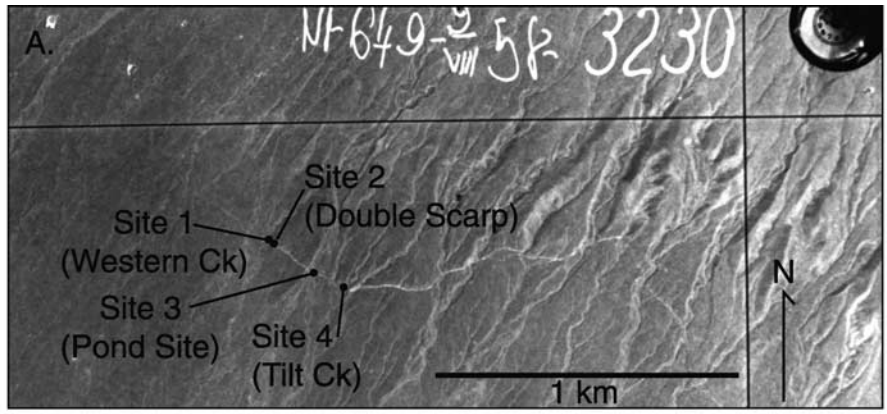

52%

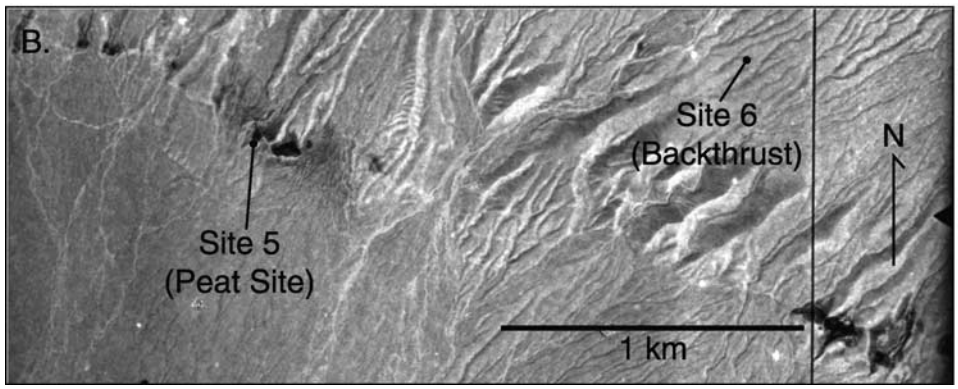

Figure 4. Aerial photographs showing locations of excavation sites. Photographs taken in 1958 by Russian team shortly after the Gobi Altay earthquake. Fresh scarps show up as bright white lines crossing drainages. A. Western sites, 1–4, located on photo number 3230. B. Sites 5 and 6 located on photo number 3032.

[15] Deposits in the upper plate of fault F2, which overrode the ground surface in 1957, are composed of massive, unsorted colluvium produced in response to prehistoric earthquakes. Two distinct colluvial units, C2 and C3, represent deposits associated with the penultimate and the prepenultimate events, respectively. Units C2 and C3 are faulted by faults F1 and F2, both of which were active in 1957. Fault F3 also offsets a colluvial unit, C2a, which we correlate with unit C2.

[16] Further evidence that prehistoric earthquakes have affected these deposits are the relations that show the soil developed in unit 10 has been erosionally stripped between meters 1.5 and 4. The dashed line between meters 4 and 8 in unit 10 defines the lower limit of a darkening zone associated with pedogenic processes. South of meter 4 this weak soil horizon is absent. Some erosion of this horizon has occurred since 1957, but the amount of stripping is more than can be attributed to post-1957 erosion. We base this conclusion on the small size of the post 1957 colluvium produced in response to slip on fault F3 (C1a, Figure 7). Thus the erosion of unit 10 provides additional evidence of pre-1957 surface faulting at this site.

[17] We interpret that colluvial units C2 and C2a were deposited in response to the penultimate surface rupture, and offsets of these deposits must be attributed to the 1957 event. Therefore, the distances along fault F1 between B and B′ (14 cm), and along fault F3 between C and C′ (80 cm) are minimum values of 1957 dip slip on each structure. Restoring the 1.6 m of offset on the unit 10/unit 20 contact across fault F3 (D–D′) provides an estimate of the total slip on F3 from both the 1957 and the penultimate earthquakes. Subtracting the 1957 slip (C–C′, 80 cm) from this total gives a minimum estimated slip of about 80 cm for the penultimate event. Combining the 1957 slip on faults F1, F2, and F3 gives a minimum estimate of 1957 fault slip at this site of 2.94 m.

[18] We collected two samples for luminescence dating from this exposure. Sample OSL9, collected from unit C3, did not provide reliable age data: multiple OSL measurements on quartz grains yielded widely disparate age estimates. Sample OSL1, collected from the silt cap on the alluvial fan sediment, yielded an age estimate of 26.6 ± 2.1 ka or 16.1 ± 2.0 ka (Table 1). The age ambiguity for sample OSL1 is the result of luminescence measurements made at different temperatures (Table 1), and it is not possible to determine which age is correct (G. Berger, personal communication, 1999). We interpret the silt cap to be an eolian dust deposit that accumulated on the abandoned T3 surface; therefore its age is a minimum estimate for the age of the abandonment of the T3 surface. This is the same fan surface as that where site 1, Western Creek, is situated. If this age is correct, then based on the relations documented at site 1, a

Table 1. TL and IR OSL Data for OSL Samples 1–3 Analyzed at the Desert Research Institute, Reno, NV

Sample Number	Mode[a]	Preheat[b]	Bleach[c]	D_E,[d] Gy	Temperature/Time[e]	Age,[f] ka
OSL1 (site 2, Figure 7)	TL	125 °C/3d	TB/560(3d)	53.7 ± 7.1	210–280 °C	13.5
	TL	125 °C/3d	TB/400(3d)	65.6 ± 7.8	210–270 °C	16.5
	TL	125 °C/3d	TB/400(3d)	93 ± 13	310–380 °C	23.4
	IR OSL	135 °C/3d	TB/780(4h)	63.9 ± 7.0	1–50 s	**16.1 ± 2.0**
	IR OSL	155 °C/3d	TB/780(4h)	105.8 ± 7.3	1–5 s	**26.6 ± 2.1**
OSL2 (site 4, Figure 9)	TL	125 °C/3d	TB/560(3d)	53.5 ± 5.1	250–320 °C	14.9
	TL	125 °C/3d	TB/400(3d)	71.7 ± 6.7	220–370 °C	20.0
	IR OSL	135 °C/2d	TB/780(3h)	45.8 ± 2.5	1–25 s	12.7
	IR OSL	155 °C/2d	TB/780(3h)	43.7 ± 3.3	1–10 s	12.1
				45.0 ± 2.0		**12.5 ± 0.8**
OSL3 (site 4, Figure 9)	IR OSL	135 °C/2d	TB/780(3h)	17.2 ± 1.8	1–15 s	5.29
	IR OSL	155 °C/2d	TB/780(3h)	20.8 ± 1.9	1–10 s	6.40
				18.9 ± 1.8		**5.8 ± 0.6**

[a]For all TL runs, the heating rate was 5 °C/s. The polymineralic 4–11 μm size fraction was used for all TL measurements. Both TL and IR OSL were detected at the 420 ± 20 nm spectral region (bandpass 390–470 nm at 1% cut).
[b]The chosen prereadout annealing (see *Berger* [1994] and *Ollerhead et al.* [1994] for rationale).
[c]Values in parentheses specify optical bleaching time. TB = total-bleach method. Different optical-filter bandpass regions were used for bleaching, as follows: 560 = 560–800 nm at 10% cut; 400 = 390–740 nm at 5% cut; Hg = full-spectrum Hg "sunlamp"; 780 = >780 nm solar spectrum passed.
[d]Weighted mean equivalent dose plus average error over temperature or time interval in next column. A weighting-saturating-exponential regression model [*Berger et al.*, 1987] or a weighted-exponential-plus-line regression model [*Berger*, 1990b] was employed for all samples.
[e]The readout temperature (TL) or readout time (IR OSL) interval for which D_E is calculated.
[f]Bold type indicates final age estimates.

minimum of five earthquakes have occurred during the last 26.6 ± 2.1 ka or 16.1 ± 2.0 ka. We see evidence for only three of these earthquakes at site 2. There are several possible reasons for this: it is possible that some of the colluvial packages identified at site 1 were deposited in response to climatic change, rather than in response to renewal of the scarp. Alternatively, because we were unable to extend our trench farther northward at site 2, we may not have exposed the entire fault zone, and it is possible that our trench was not long enough to expose the evidence for all of the events.

[19] **Site 3 (Pond site)** is approximately 180 m southeast of site 2 (Figure 5), where we hand-excavated a trench into terrace surface T2. Surface T2 is inset into and therefore younger than the T3 fan surface, and this age difference is reflected in the younger age of OSL6, collected from terrace deposits at this site (4.1 ± 0.3 ka, Table 2), versus OSL1 collected at site 2 (≥16.1 ± 2.0 ka, Table 1). Two fault zones ruptured here in 1957, and the area between the two was tilted to the northeast creating a region where post-1957 sediment is being ponded (Figure 8). We interpret the colluvial units C1 and C1a, which are not faulted, as forming in response to the 1957 earthquake. A small 1957 free face is still visible adjacent to F1 between meters 8 and 9.

[20] An older massive and unsorted colluvial deposit, C2, is faulted by F1, overrides the 1957 ground surface, and stands out in contrast to the bedded alluvial units. We interpret unit C2 as colluvium from the penultimate event associated with rupture of the F2 fault strands. Unit C2 was subsequently faulted in 1957 by the rupture of fault F1. The buried free face associated with the penultimate event is preserved between meters 9 and 10. We correlate unit 20 with colluvial unit C2.

[21] The hatchured areas beneath units C1, C2 (between meters 5 and 10), and 40 (between meters 0 and 2) represent the ground surface at the time of the 1957 earthquake. This horizon is marked by vesiculation of the sediment and pedogenic darkening. Several small clumps of dead grass have been buried by C1 or overridden by the upper plates of faults F1 and F3. Restoring the former ground surface across fault F1 (A–A′) gives a minimum of about 1 m of

Table 2. GSL and IR OSL Data and Ages for Samples OSL 6–14 Analyzed at UC Riverside[a]

Sample Number	Size, μm	Paleodose (D_E), Gy	Dose Rate, mGy yr^{-1}	Age, ka
OSL6 (site 3, Figure 8)	90–125	10.49 ± 1.34	2.58 ± 0.11	**4.1 ± 0.3** (Quartz)
OSL8 (site 3, Figure 8)	90–125	6.99 ± 0.89	2.65 ± 0.17	**2.6 ± 0.2** (Quartz)
OSL9 (site 2, Figure 7)	90–125	5.95 ± 2.57	3.01 ± 0.19	0.6–3.1 (Quartz)
OSL10 (site 6, Figure 12)	125–180	10.69 ± 0.68	3.87 ± 0.26	**2.8 ± 0.2** (Quartz)
OSL12 (site 5, Figure 10)	90–125	7.12 ± 0.54	3.17 ± 0.13	**2.3 ± 0.2** **3.2 ± 0.4*** (Quartz)
OSL13 (site 5, Figure 11)	90–125	18.66 ± 1.74	6.67 ± 0.40	5.9 ± 0.7 8.1 ± 1.3* (Feldspar)
OSL14 (site 5, Figure 11)	90–125	21.21 ± 2.02	3.63 ± 0.15	**5.8 ± 0.4** **7.7 ± 0.9*** (Quartz)

[a]Asterisks indicate age estimate calculations based on the assumption of completely saturated field conditions. Bold typeface indicates age estimates that are statistically reliable (i.e., those that have consistent repeat values of D_E and therefore are completely bleached).

Table 3. Dosimetry Data For Luminescence Samples[a]

Sample (OSL-)	Water[b]	K_2O, wt.% (±0.05)	Th, ppm	U, ppm	Dose Rate, Gy kyr^{-1}
1[c]	0.10 ± 0.03	2.83	8.65 ± 0.99	3.27 ± 0.30	3.97 ± 0.16[d]
		2.50	6.93 ± 0.50	2.99 ± 0.25	3.97 ± 0.17[d]
2[c]	0.08 ± 0.03	2.09	4.76 ± 0.68	3.20 ± 0.21	3.60 ± 0.17[d]
		2.26	5.62 ± 0.70	2.32 ± 0.23	
3[c]	0.10 ± 0.03	1.96	6.56 ± 0.89	2.49 ± 0.27	3.25 ± 0.17[d]
6[e]		1.59	5.43 ± 0.26	2.03 ± 0.11	2.80 ± 0.21 (f)[f]
	0.030				2.58 ± 0.11 (q)
7[g]	0.055	1.82	7.88 ± 0.79	1.87 ± 0.19	3.31 ± 0.26 (f)[f]
					2.78 ± 0.17 (q)
8[g]	0.056	1.72	6.89 ± 0.69	1.47 ± 0.15	3.03 ± 0.22 (f)[f]
					2.65 ± 0.17 (q)
9[g]	0.069	1.93	9.34 ± 0.93	1.57 ± 0.16	3.37 ± 0.23 (f)[f]
					3.01 ± 0.19 (q)
10[g]	0.029	2.54	10.8 ± 1.08	1.95 ± 0.20	4.24 ± 0.31 (f)[f]
					3.87± 0.26 (q)
12[e]	0.049	1.83	7.58 ± 0.26	2.67 ± 0.11	5.09 ± 0.31 (f)[f]
					3.17 ± 0.13 (q)
13[e]	0.043	2.18	13.58 ± 0.39	4.43 ± 0.17	6.67 ± 0.40 (f)[f]
14[e]	0.045	2.17	9.31 ± 0.25	3.06 ± 0.08	5.61 ± 0.34 (f)[f]
					3.63 ± 0.15 (q)

[a]Samples 1–3 were analyzed at the laboratory of Glenn Berger, Desert Research Institute. All other samples were analyzed at the laboratory of Lewis Owen, University of California, Riverside. The different laboratories use differing reporting conventions, which is reflected in the different parameters listed below for each set of samples.

[b]Assumed ratio of weight of water/weight of dry sample, based on measured values for as-collected and saturation conditions. Uncertainties are ±1σ.

[c]The determination of radionuclide concentrations from thick-source-alpha-particle-counting (TSAC) method [*Huntley and Wintle*, 1981].

[d]Calculated with the conversion factors and equations given by *Berger* [1988], and includes a cosmic ray component of 0.10 ± 0.02 estimated from the data of *Prescott and Hutton* [1988].

[e]The determination of radionuclide concentrations using gamma ray spectrometer with sodium iodide crystal (Shannon Mahan, personal communication, 2001).

[f]Dose rate conversion factors from *Adamiec and Aitken* [1999]; cosmic dose rate is derived from *Prescott and Hutton* [1988] for each site. Dose rates for K-feldspar (f) and quartz (q).

[g]The determination of radionuclide concentrations using nuclear activation analysis (NAA) method, measurement using high-resolution gamma ray spectrometer.

Table 4. Calculated Dates From ^{14}C Analysis of Charcoal and Paleosols Reported by Rafter Radiocarbon Laboratory, Wellington, New Zealand

No.	Sample (Field No./Lab No.)	$\delta^{13}C$, ‰	^{14}C age,[a] yr B.P.	Calendar Date,[b] A.D. If Unlabeled	Calibrated Years B.P.	Material
RC1	M97DS1/NZA 8074	−23.6	189 ± 69	1630–1950 (.97)	0–320 (.97)	grass
	Double Scarp trench (Figure 7)			1530–1560 (.03)	390–420 (.03)	
RC2	Peat 4/NZA 8068	−23.7	226 ± 66	1490–1950 (1.00)	0–460 (1.00)	charcoal
	Peat site trench (Figure 10)					
RC3	Peat 5/NZA 8069	−24.2	383 ± 78	1410–1660 (1.00)	300–530 (1.00)	charcoal
	Peat site trench (Figure 10)					
RC4	Peat 3/NZA 8067	−24.0	427 ± 71	1400–1640 (1.00)	310–550 (1.00)	charcoal
	Peat site trench (Figure 10)					
RC5	Peat 9/NZA 8275	−28.8	5128 ± 68	3710–4220 B.C. (1.00)	5660–6170 (1.00)	organic horizon
	Peat site trench (Figure 10)			3760–4050 B.C. (.98)	5710–6000 (.98)	
RC6	Pit D/NZA 8049	−23.3	5752 ± 71	4450–4730 B.C. (.96)	6400–6680 (.96)	charcoal
	Peat site soil pit (Figure 11)			4750–4770 B.C. (.04)	6700–6720 (.04)	
RC7	Pit E-1/NZA 8034	−21.7	6180 ± 69	4940–5300 B.C. (1.00)	6890–7250 (1.00)	charcoal
	Peat site soil pit (Figure 11)					
RC8	Pit E-2/NZA 8091	−24.7	6260 ± 70	5000–5370 B.C. (1.00)	6950–7320 (1.00)	organic horizon
	Peat site soil pit (Figure 11)					
RC9	Peat 7/NZA 8119	−28.5	6212 ± 78	4940–5320 B.C. (1.00)	6890–7270 (1.00)	organic horizon
	Peat site trench (Figure 10)					
Avg 7, 8, 9[c]				5060–5300 B.C. (1.00)	7010–7250 (1.00)	
RC10	Pit H/NZA 8050	−23.1	9078 ± 72	7970–8530 B.C. (1.00)	9920–10,480 (1.00)	charcoal
	Peat site soil pit (Figure 11)			8200–8480 B.C. (.91)	10,150–10,430 (.91)	

[a]Calculations assume a Libby half-life (5568 years). Uncertainties are 1 standard deviation counting errors.

[b]Dendrochronologically calibrated, calendar age ranges using the data set of *Stuiver et al.* [1998], Method B, with 2 standard deviation uncertainty. Calibrated using CALIB Rev. 4.3 [*Stuiver and Reimer*, 1993]. Age ranges are rounded off to the nearest decade. Numbers in parentheses represent relative area under probability distribution.

[c]Weighted average of RC7, 8, and 9, calculated using Calib 4.3.

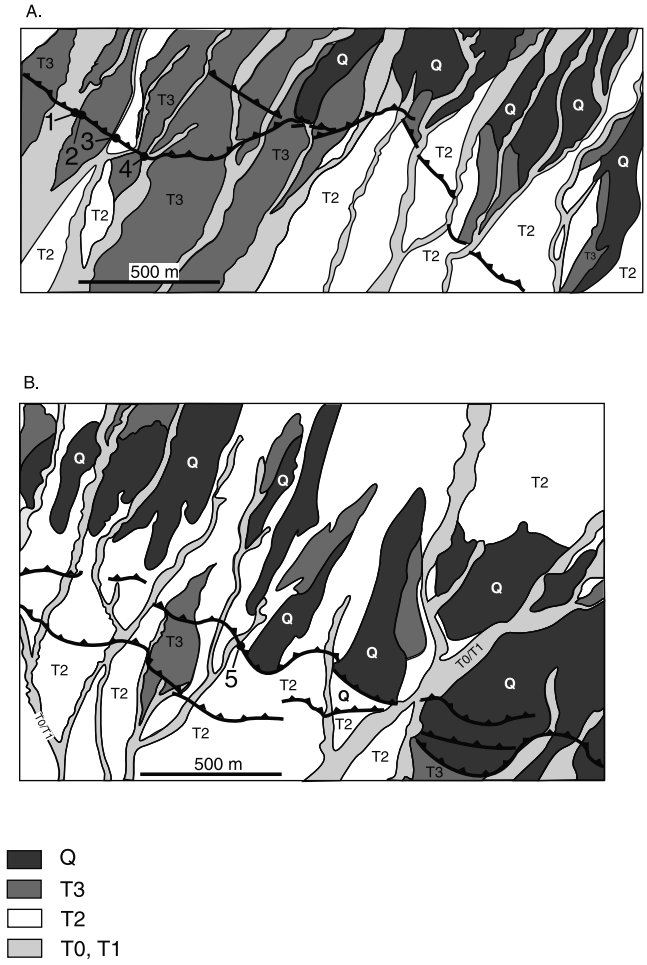

Figure 5. Map showing geomorphic surfaces and 1957 fault ruptures based on interpretation of aerial photographs and reconnaissance field mapping. Heavy lines are 1957 fault scarps, teeth on upper plate. T0/T1 = modern streams and lowest terrace (T1), which can not be distinguished at this scale. T2 = terrace 2; T3 = terrace 3; Q = Older alluvium: remnants of fans that have been folded and dissected to the point where no original alluvial surface remains. Solid circles are study sites 1–5. A. Map of western region near sites 1–4. B. Map of region near sites 5 and 6 (Site 6 is off map approximately 200 m to the east).

1957 dip slip. Taking into consideration that only the 1957 earthquake has faulted the penultimate colluvial unit, C2, increases this slip estimate to 1.4 m (A–A″). Slip on fault F3 can be estimated using two sets of piercing points: the overridden 1957 ground surface (B–B′) and the unit 10/unit 20 contact (C–C′). Both indicate about 1 m of slip across F3. Therefore, the total minimum estimated dip slip at this site in 1957 is about 2.4 m.

[22] Two luminescence samples were analyzed from this site, samples OSL6 and OSL8 (Table 2). Sample OSL6 from the silt cap overlying the alluvial fan sequence (unit 30) yielded an age of 4.1 ± 0.3 ka, and predates the penultimate earthquake. This age is also a minimum estimate for the abandonment of the T2 terrace surface. Sample OSL8 from unit 20, which we correlate with unit C2, the penultimate colluvial wedge, yielded an age of 2.6 ± 0.2 ka. If this correlation is correct, then these relations indicate that the penultimate surface-faulting event occurred before 2.6 ± 0.2 ka.

[23] **Site 4 (Tilt Creek)** is a 3-m-high natural stream cut approximately 100 m southeast of site 3 that exposes T3 alluvial-fan gravel and colluvial deposits derived from the fault scarp (Figure 9). The alluvial gravel is tilted to the southwest on the northeast side of the fault zone. Southwest of the fault zone, we distinguish the colluvial deposits from the alluvial fan gravel by their redder color, siltier texture, and massive, unsorted character.

[24] Units 10–40 are alluvial fan deposits that have been disrupted across a zone that contains five faults. Faults F1 and F2 moved during the 1957 earthquake, displacing all units except unit C1, which was deposited in response to this event. An older colluvial deposit, unit C2, which we interpret to have been deposited in response to the penultimate earthquake, was faulted during the 1957 earthquake. The penultimate earthquake included rupture of faults F4 and F5, which bound an area of internally sheared small-pebble gravel. Faults F4 and F5 break an older colluvial deposit, unit C3, which we interpret as having formed in response to the prepenultimate event.

[25] Two samples for luminescence dating from this site, OSL2 and OSL3 (Table 1), yielded ages of 12.5 ± 0.8 ka and 5.8 ± 0.6 ka, respectively. These ages are not in correct stratigraphic order, indicating that at least one of them is incorrect. Because luminescence dates are more likely to give erroneously old ages in this depositional environment [*Aitken*, 1985], we infer the age of OSL2 to be incorrect. Unit C3 predates the penultimate event, and the age of sample OSL3, 5.8 ± 0.6 ka, is consistent with the other prepenultimate luminescence dates from sites 2 and 3. OSL3 also postdates the prepenultimate event.

2.2. Site 5 (Peat Site)

[26] Only site 5 (Peat site), located about 3.5 km southeast of site 1 (Figures 4B and 5B), provided a significant amount of material for radiocarbon dating. This site is located on an inset terrace surface that occupies the same geomorphic position as terrace T2, but lies within a different alluvial fan system, and therefore the two surfaces may not be coeval. Springs in this area provide favorable conditions for the formation of organic-rich horizons, which are interbedded with alluvial gravel and fine-grained sediment. We excavated a hand-dug trench across the northernmost of two subparallel fault zones that ruptured at this longitude during the 1957 earthquake (Figures 10A and 10B). We also dug a pit into the alluvial surface (T2) about 5 m north of the end of the trench to collect additional samples for radiocarbon and luminescence analyses (Figure 11).

[27] The log of the trench exposure shows a complex zone of deformation more than 14 m wide (Figure 10). Although the stratigraphic relations are complicated, we see clear evidence for at least two earthquakes: the 1957 earthquake and one earlier event. In addition, there is some evidence to suggest a third event. We found no piercing points useful for measuring dip slip on any of the major faults. The darkened and hatchured regions on the log show buried, dark, organic-rich horizons (designated OH) that mark former ground surfaces. This sedimentary section records the transition from alluvial-fan sedimentation, the

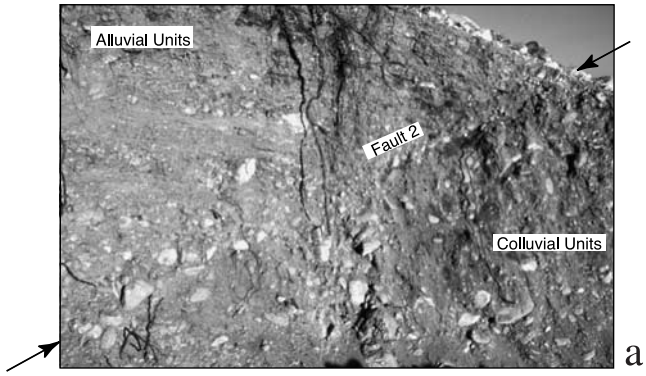

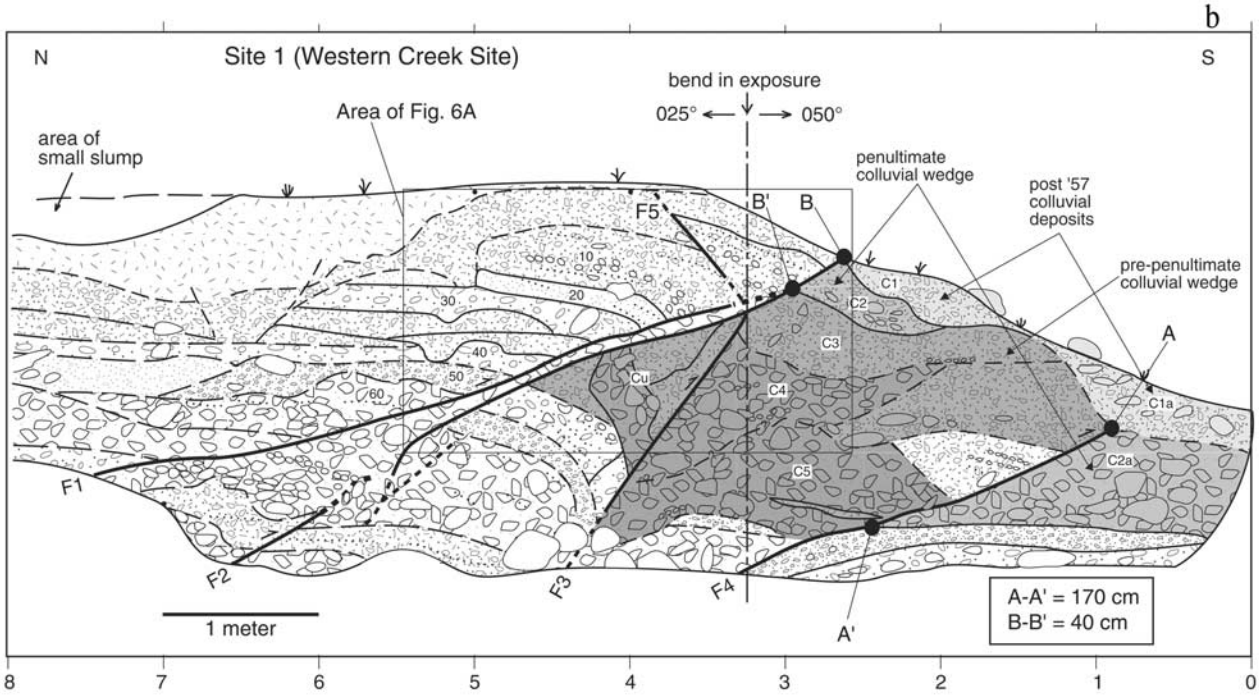

Figure 6. A. Photograph of part of site 1 (Western Creek, eastern wall), a cleaned stream cut, showing contrast between alluvial units and colluvial units across one of the principal fault strands. B. Log of site 1 (Western Creek). Exposed in the stream bank are alluvial fan deposits and colluvial units disrupted by a complex zone of thrust and reverse faults. Shaded regions denote colluvial materials that we interpret as forming in response to scarp-forming earthquakes. We recognize a minimum of five colluvial units (C1–C5) at this site that postdate the abandonment of the fan surface. All colluvial units except C1 are faulted. We interpret C2–C5 to have formed in response to prehistoric ruptures of this fault zone. A–A′ and B–B′ represent minimum amounts of fault slip in 1957, totaling 2.1 m. C. Explanation of symbols used for this and all other logs.

gravels, sands and silts below organic horizon E, to sheetwash and postabandonment eolian sedimentation dominated by deposition of silts.

[28] Faults F1 and F2 (Figure 10) extend nearly to the present ground surface, which indicates that slip occurred on these faults in the 1957 earthquake. Unit 1, an unsorted, massive, pebbly silt, has been deposited since the 1957 earthquake, and is undeformed; it buries clumps of grass that mark the 1957 ground surface (Figure 10, near meters 14, 13, and 11). An interesting element of the 1957 rupture is fault F1, a backthrust that breaks through a small, local unit, labeled unit 3, between meters 8 and 9. This unique deposit contains a high concentration of charcoal on the upthrown (south) side of F1 on the eastern wall of the excavation. On the downthrown (north) side of F1, the correlative unit contains very little charcoal. This abrupt facies change across the fault indicates a component of strike-slip displacement. On the western wall of the excavation, the high concentration of charcoal is present on the downthrown side of the fault, and not on the upthrown side. The trench wall is nearly perpendicular to the fault plane, and therefore purely dip-slip motion across the fault could not produce this juxtaposition of different facies. These relations require a component of strike slip, and indicate that a minimum of

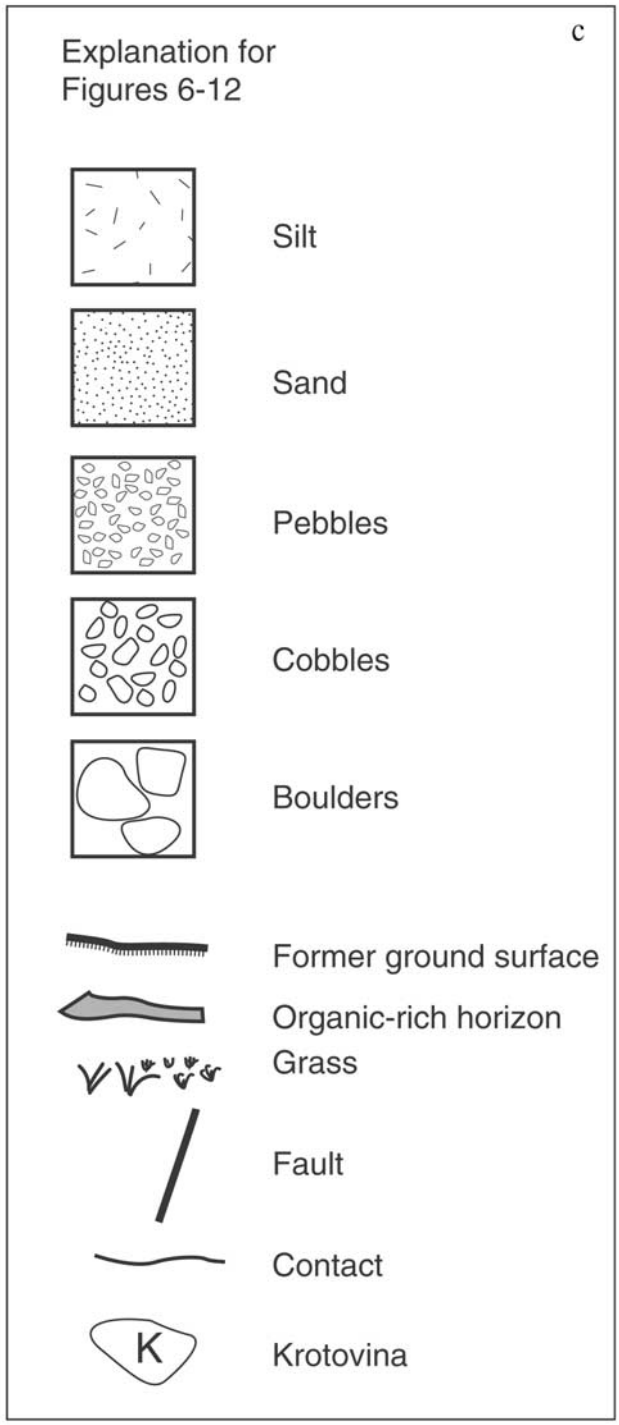

Figure 6. (continued)

about 1 m of left-lateral slip occurred on fault F1 in 1957. The young age of unit 3, less than 600 years B.P. (samples RC2, 3, and 4, Figure 10, Table 4), and its limited extent suggests that it could represent an ancient fire built by local inhabitants.

[29] Evidence of the penultimate event at this site includes the upward termination of numerous secondary faults and fissures. Unit 6, which we correlate with OH C, is an organic horizon present in the southern part of the excavation between meters 2 and 6, which has been intensely deformed. A series of fractures and faults breaks through unit 6 (OH C) and into unit 5, but not into overlying unit 4. We interpret these faults and fractures as evidence of faulting during the penultimate earthquake, which occurred sometime after the deposition of units 6 (OH C) and 5. Some of these faults show a component of normal separation. This apparent normal slip could be due either to extension within the hanging wall of a thrust fault, to strike-slip displacement of nonhorizontal beds, or to normal displacements on right-stepping en echelon secondary faults due to left-lateral motion along the main fault.

[30] Additional evidence for the penultimate event is present near the northern end of the trench (meters 13–15) where a set of fractures breaks up to the top of organic horizon B, but does not extend into the overlying deposits. Similarly, a fissure between meters 9 and 10 also terminates at this stratigraphic level. Additional stratigraphic evidence suggesting that this event occurred prior to the deposition of unit 4 is the thickness change of this unit. On the downthrown side of the fault unit 4 is up to 30 cm thick, and pinches out abruptly near the fault zone, suggesting that the presence of a fault scarp may have influenced its deposition. The age of the penultimate earthquake at this site is constrained by the radiocarbon age of unit 6 (RC5, Table 4) to be younger than about 6000 years B.P.

[31] Two features in this excavation suggest the occurrence of a third earthquake prior to the penultimate event. Faults F3 and F4 break through organic horizon E, but both terminate below unit 5. If these faults represent a third earthquake, then the radiocarbon age of organic horizon E provides a maximum age constraint of 7.3 ka (RC7, 8, and 9, Table 4). Two additional faults, F5 and F6 near meter 16 may represent earlier events. However, we have little evidence to support the occurrence of possible earlier events, and no data to constrain their ages.

[32] A hand-dug pit on the alluvial surface about 5 m north of the end of the trench provided us with a more complete understanding of the alluvial stratigraphy, and provided additional samples for both radiocarbon and luminescence dating (Figure 11). Few horizons in the trench were suitable for dating, and the additional exposure provided better samples for age analyses. Radiocarbon ages of bulk samples from horizons in the pit (Figure 11; Table 4) show a consistent age progression in stratigraphic order from oldest (9.9–10.3 ka) to youngest (6.4–6.7 ka) (Table 4). Two samples were analyzed from organic horizon E in the pit: A bulk sample yielding an age of 7.0–7.3 ka, and a charcoal sample extracted from the bulk sample, which yielded an age of 6.9–7.3 ka. These two ages are indistinguishable.

[33] Relations in the trench indicate that the age of organic horizon E establishes a maximum age for the prepenultimate event. A bulk sample of organic horizon E collected in the trench (meters 15–16, Figure 10) yielded a radiocarbon age of 6.9–7.3 ka (Table 4), indistinguishable from the pit samples, and thus confirming our correlation of this unit between the trench and the pit. The average age of these three samples is 7.0–7.3 ka. The radiocarbon dates and stratigraphic relations allow us to correlate several key units between the pit and the trench, and across the fault zone in the trench.

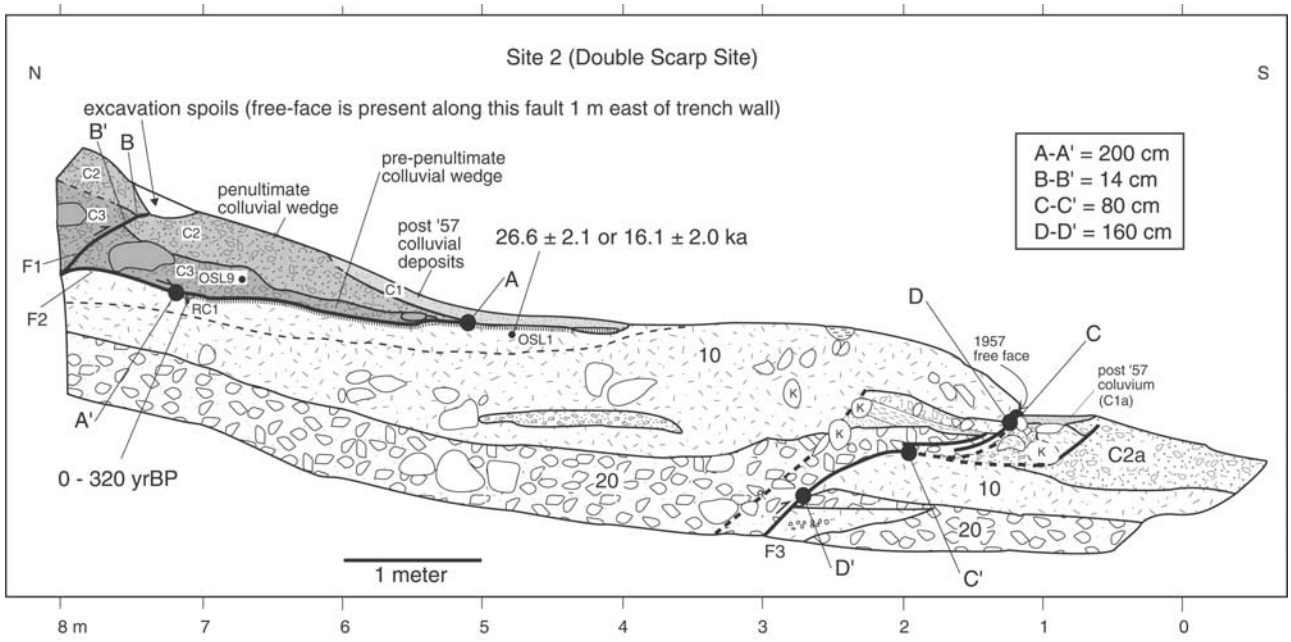

Figure 7. Log of site 2 (Double scarp, eastern wall). Shaded units are colluvial units we interpret as forming in response to scarp-forming earthquakes. C1 is unfaulted, and formed in response to the 1957 earthquake. C2 and C3 formed in response to two earlier earthquakes. The luminescence age of OSL1 (Table 1) provides a minimum estimate of the time since the T3 surface was abandoned. The radiocarbon age of RC1 (Table 4) shows that this grass was overridden by C3 and C2 during the 1957 earthquake. A–A′, B–B′, and C–C′ represent minimum amounts of 1957 fault slip, totaling 2.94 m. D–D′ represents cumulative slip in 1957 and the penultimate event on fault F3, suggesting a minimum of 80 cm of slip on this fault strand during the penultimate event.

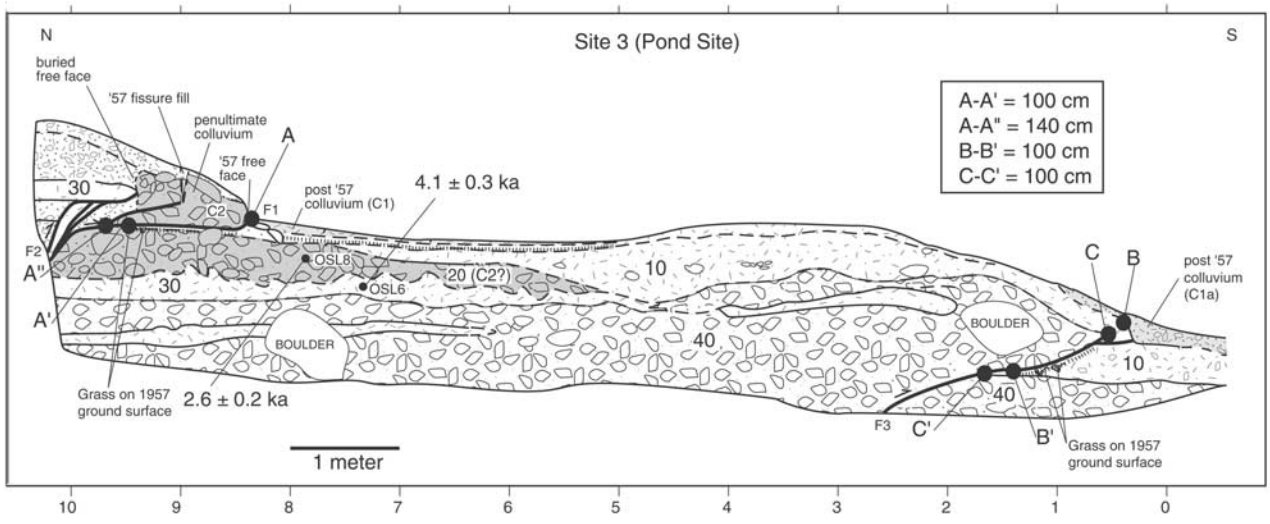

Figure 8. Log of site 3 (Pond site, western wall. Log has been reversed to show an east-facing view.) Shaded units are colluvial units we interpret as forming in response to scarp-forming earthquakes. C1 is unfaulted, and formed in response to the 1957 earthquake. C2 formed in response to the penultimate earthquake. The luminescence age of OSL8 (Table 2) indicates that the penultimate earthquake occurred prior 2.6 ± 0.2 ka. OSL6 indicates the penultimate earthquake occurred after 4.1 ± 0.3 ka. This sample also provides a maximum estimate for the age of T2. Dead grass under fault 1 indicates a minimum displacement (A–A′) of about 1 m across fault 1 in 1957. The minimum offset of C2, A–A″, provides a better estimate of 1.4 m. B–B′ (1957 ground surface) and C–C′ (unit 10/unit 40 contact) both provide estimates of 1957 slip across fault 3 of about 1 m.

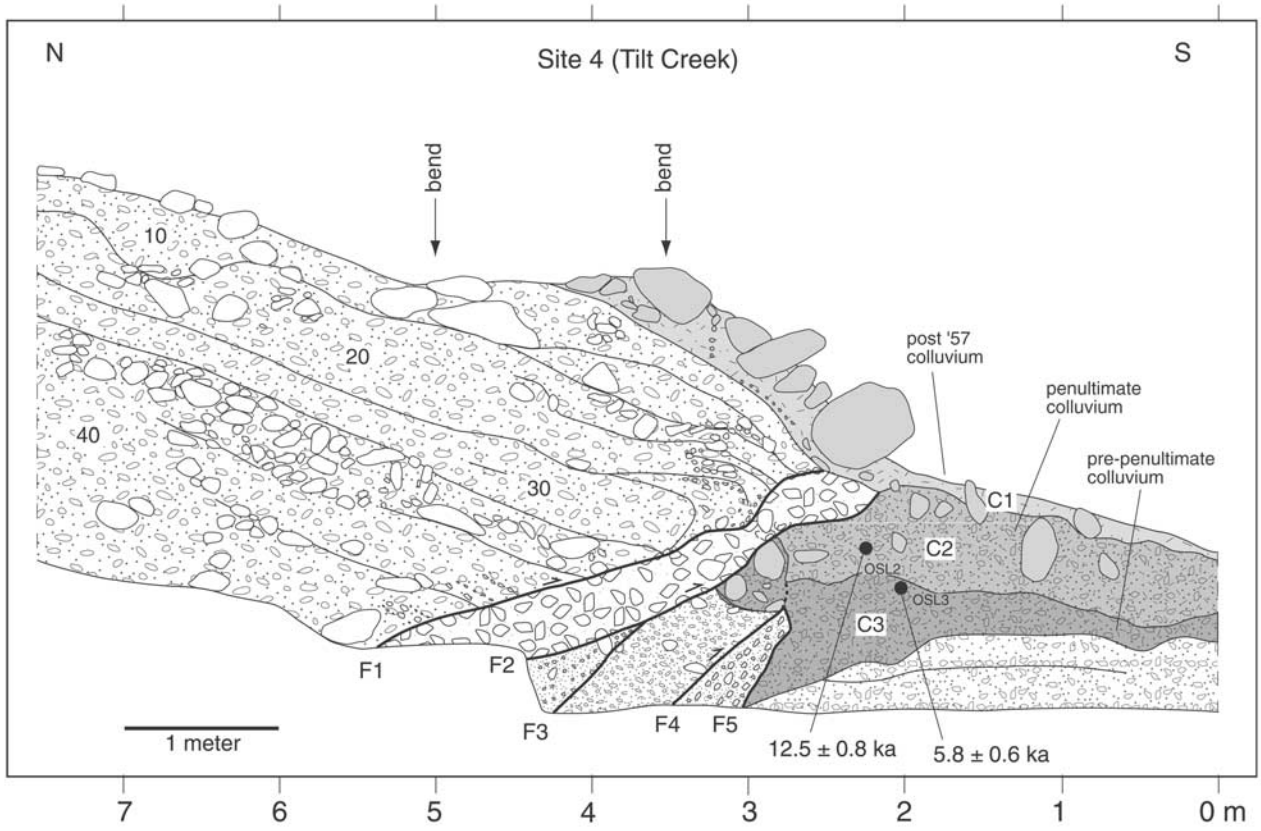

Figure 9. Log of Site 4 (Tilt Creek, western wall. Log has been reversed to show an east-facing view.) Shaded units are colluvial units we interpret as forming in response to scarp-forming earthquakes. C1 is unfaulted, and formed in response to the 1957 earthquake. C2 formed in response to the penultimate earthquake, and C3 formed in response to the prepenultimate, or third event back. The luminescence age of OSL3 (Table 1) indicates that the penultimate event occurred after 5.8 ± 0.6 ka, and the third event back occurred prior to this date. We believe the analysis of OSL2 (Table 1) yielded an incorrect age.

[34] In addition to radiocarbon samples, we collected samples for OSL dating in both the pit (OSL13, OSL14) and the excavation (OSL12). We discuss these luminescence ages and their relationship to the radiocarbon ages below, in the section on age data.

2.3. Site 6 (Backthrust Site)

[35] Site 6 is approximately 0.6 km north of the main Gurvan Bulag rupture on an alluvial surface that is higher and older than the T3 fan surface (Figure 4). At this location, the surface is deformed by a subsidiary backthrust. A free face associated with the 1957 earthquake is present along strike within 10 m of the site, showing that this structure ruptured during the 1957 earthquake. We chose this site to study because the uphill-facing scarp would trap sediment that might record evidence of prehistoric earthquakes (Figure 12). Units 10–30 are alluvial-fan deposits, and units C1 and C2 are colluvial deposits associated with the fault scarp. Unit C1 is not faulted, and represents deposition that has occurred since the 1957 earthquake. Unit C2 is faulted, and therefore predates the 1957 event. We interpret this unit as having formed in response to the penultimate earthquake that ruptured this structure. One luminescence sample, OSL10, was analyzed, yielding an age of 2.8 ± 0.2 ka (Table 2). This sample was collected from C2, and therefore postdates the penultimate earthquake.

[36] Unit C2 is offset 50 cm (A–A′), which represents dip slip on this fault in 1957. The offset of the unit 10/unit 20 contact (A–A″) is about 1 m, which represents the cumulative dip slip in 1957 and the penultimate event. Thus the 1957 earthquake and the penultimate event produced similar amounts of dip slip on this fault.

3. Luminescence and Radiocarbon Ages

[37] The radiocarbon samples collected from site 5 (peat site) provide our most reliable ages. The ages of all samples are consistent with one another, and multiple samples from the same unit (organic horizon E) yielded indistinguishable ages (Figures 10 and 11; Table 4). Because detrital charcoal always yields an age greater than that of the sediment in which it is deposited, there is necessarily some uncertainty regarding the actual age of the deposits. However, the absence of stratigraphic reversals or variation in the ages of multiple samples within the same unit suggests that the detrital charcoal is not significantly older than the deposits. Therefore, we assume the radiocarbon ages closely reflect the time of deposition of the stratigraphic units.

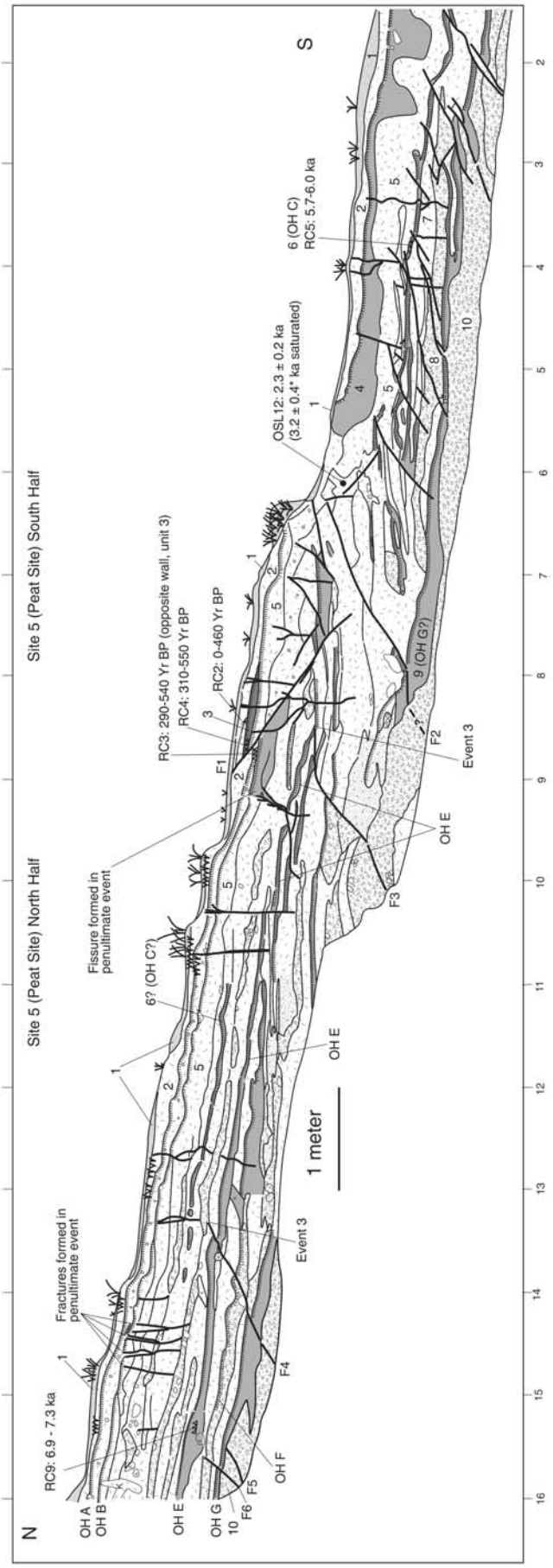

Figure 10. Log of site 5 (Peat site, eastern wall). Shaded and hachured areas represent former ground surfaces marked by accumulation of organic material (OH = Organic Horizon). Lightly shaded horizon (unit 1) is material that has accumulated since the 1957 earthquake. Faults 1 and 2 ruptured in 1957. Numerous small faults in south part of trench break into unit 5 but not above, and represent the penultimate earthquake. The penultimate earthquake is also represented by a fissure and several fractures in unit 5 within the northern part of the trench. Faults 3 and 4 provide evidence of a third event. All three events have occurred since the formation of organic horizon E, radiocarbon dated at 7.0–7.3 ka (Table 4), and the penultimate event occurred some time post the formation of unit 6, radiocarbon dated at 5.7–6.0 ka (Table 4). Queries indicate uncertainty in the correlation of units across the fault zone and between the trench and the pit (Figure 11).

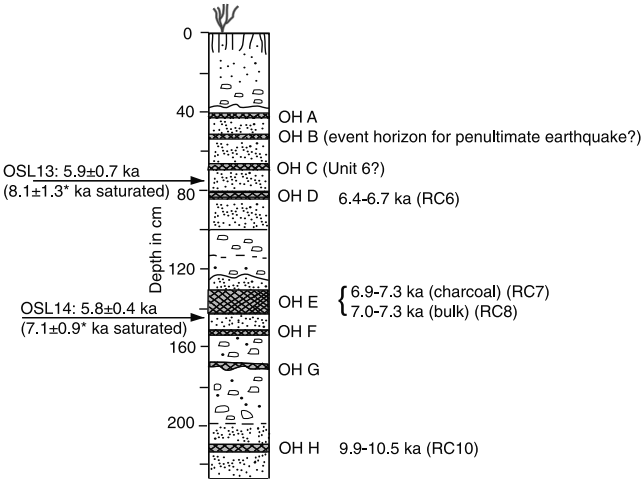

Figure 11. Log of pit dug into the T2 surface about 5 m north of the site 5 trench (shown in Figure 10). Radiocarbon samples (Table 4) indicate section accumulated over the last approximately 10 kyr. Luminescence age (OSL14) is anomalously young and inconsistent with the radiocarbon ages. We believe this is due to the effects of groundwater at this site. Age estimates in parentheses and asterisked are calculated assuming completely saturated conditions. OSL13 did not yield enough quartz grains to provide an age estimate; reported age is based on measurement of feldspar grains. Queries indicate uncertainty in the correlation of units across the fault zone and between the trench and the pit.

[38] At most of the sites we did not obtain organic materials for radiocarbon analysis, and therefore we must rely on luminescence techniques to provide ages. Luminescence dating assumes that the material sampled was "reset" by sufficient exposure to sunlight at the time of deposition, and has been exposed to a constant dose of radiation from the surrounding environment since deposition [*Aitken*, 1985]. Depending on the characteristics of the mineral grains and the type of luminescence being measured, resetting the luminescence signal typically requires from a few hours to more than one day of exposure to sunlight. All of our samples from sites 2, 3, 4, and 6 were collected from colluvial wedges, a depositional environment where the sediment may not have been exposed to sunlight long enough to completely "reset" the luminescence signal. Therefore, the ages derived from these samples could be older than the age of deposition if they were not completely bleached. For samples OSL6, 8, 9, 10, 12, and 14, multiple quartz single aliquot regenerated equivalent doses (D_E) were determined that allow us to evaluate the completeness of bleaching of the sediment (Table 2). For these samples, complete bleaching is statistically indicated for all, except OSL9. The statistics of sample OSL9 indicate that there was incomplete bleaching, and thus the mean value of D_E is not likely to be representative of the sample [*Clarke et al.*, 1999]. We therefore disregard the luminescence age of this sample in our analysis. For the remaining samples (OSL 1, 2, 3, and 13) we do not have such statistics available. Sample OSL13 did not have adequate quartz content to analyze using the multiple quartz single aliquot methodology, and only a feldspar age estimate is available. Samples OSL1, 2, and 3 were analyzed in a different laboratory, using a different procedure (multiple aliquot) involving only feldspar grains, and the quality assurance was considered using

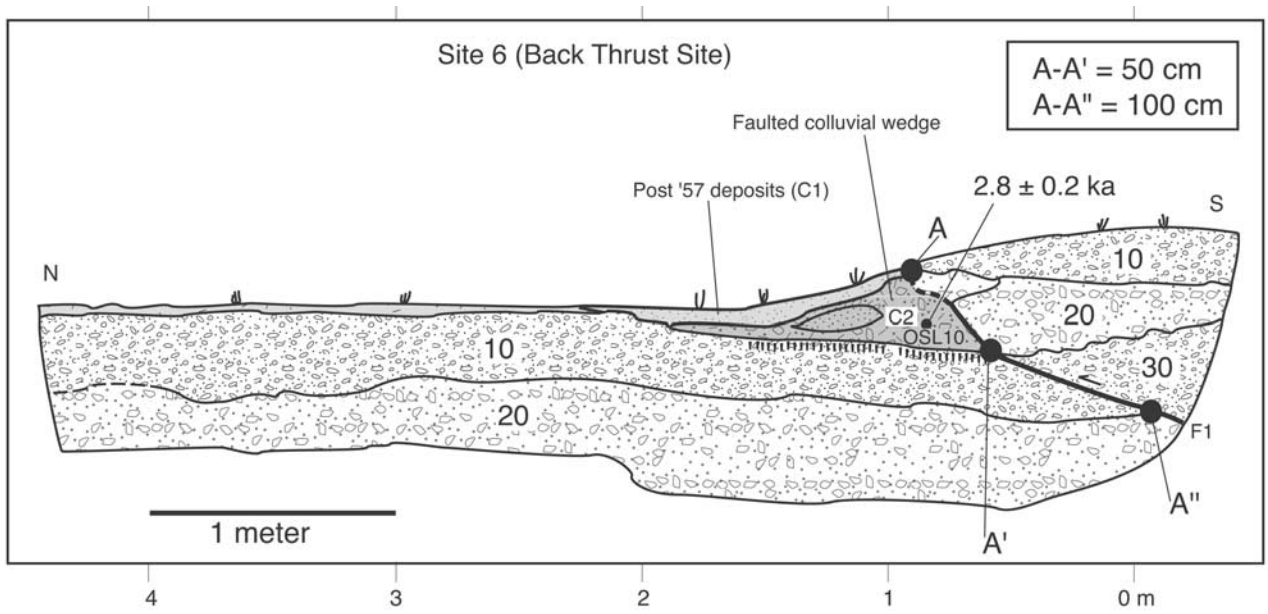

Figure 12. Log of site 6 (Backthrust). Shaded units are colluvial deposits we interpret as forming in response to scarp-forming earthquakes. C1 is unfaulted, and formed in response to the 1957 earthquake. C2 formed in response to the penultimate earthquake and was faulted in 1957. Age of sample OSL10 (Table 2) indicates penultimate event occurred prior to 2.8 ± 0.2 ka. 1957 fault slip (A–A′) is about 50 cm, and the cumulative slip in 1957 plus the penultimate event (A–A″) is about 1 m.

Table 5. Summary of Earthquakes and Age Constraints

	Site 1 (Western Creek, Figure 6)	Site 2 (Double Scarp Site, Figure 7)	Site 3 (Pond Site, Figure 8)	Site 4 (Tilt Creek, Figure 9)	Site 5 (Peat Site, Figures 10 and 11)	Site 6 (Backthrust, Figure 12)	Age Constraints on Rupture Events
Ages that postdate penultimate event			2.6 ± 0.2 ka OSL8			2.8 ± 0.2 ka OSL10	
Ages that predate penultimate event			4.1 ± 0.3 ka OSL6	5.8 ± 0.6 ka OSL3	5.7–6.0 ka RC5, RC6		Penultimate event: 2.6–4.4 ka
Ages that postdate 3rd event (prepenultimate event)				5.8 ± 0.6 ka OSL3	5.7–6.0 ka RC5		
Ages that predate 3rd event (prepenultimate event)					6.9–7.3 ka RC7, RC8, RC9		Event 3 (prepenultimate event): 5.7–7.3 ka
Five events (4 intervals)	Post T3 surface 16.1 ± 2.0 ka or 26.6 ± 2.1 ka. OSL1						Average recurrence interval of about 4 ka or 6.5 ka

comparisons to thermoluminescence (TL) age estimates of the same samples (Table 3). The ages derived from these samples (OSL 1, 2, 3 and 13) should be regarded as maximum ages, reflecting the possibility that the feldspar grains may not have been completely reset at the time of deposition.

[39] The luminescence ages derived from samples collected at sites 2, 3, 4, and 6 are consistent with each other with one prominent exception: the two samples from site 4 (Tilt Creek) are stratigraphically reversed (Figure 9). Sample OSL2 gives an age estimate of 12.5 ± 0.8 ka although it is stratigraphically above sample OSL3, which gives an age estimate of 5.8 ± 0.6 ka. We do not have multiple values of D_E to determine the completeness of bleaching for these samples, so we cannot evaluate whether the luminescence signals in these sediments were completely reset when the colluvial wedges were deposited. Because it is more likely for these deposits to yield falsely old ages than falsely young ages [*Aitken*, 1985], we interpret the age of OSL3 to represent a maximum age for unit C3, and regard the age of OSL2 to be anomalously old and incorrect. The luminescence age of OSL3 from unit C3 is consistent with the luminescence ages at the other sites and is consistent with the radiocarbon age constraints for the penultimate and prepenultimate events at site 5 (Table 5).

[40] The discrepancy between the radiocarbon ages and sample OSL14 at site 5 poses another problem (Figure 11). Site 5 is the only location where we could collect both radiocarbon and luminescence samples. Sample OSL14, with a luminescence age of 5.8 ± 0.4 ka, was collected from a unit stratigraphically below organic horizon E, which was radiocarbon dated (average of 3 samples) at 7.0–7.3 ka. There are at least two possible explanations for this discrepancy. Because detrital charcoal samples are necessarily an unknown age older than the deposits in which they are incorporated, it is possible that our radiocarbon ages are much older than the strata from which we collected them. However, the high degree of consistency among all the radiocarbon ages at site 5, especially among the three analyses from horizon E, suggests that this is not a significant problem in this case. Alternatively, it is possible that the luminescence age estimates from site 5 are too young because the calculations do not properly account for the moisture conditions during much of the duration of burial. The presence of springs in the area is a strong indication that a high groundwater table has affected the sediment at this site. These springs have been active in the past, as evidenced by the concentrations of organic materials in subsurface horizons. According to eyewitnesses, the springs were active prior to the 1957 earthquake. It is unlikely that groundwater affected sediment at any of the other sites, because no springs are present, nor is there evidence in the sedimentary record of past spring activity. If we adjust the water content used in the age calculations to reflect complete saturation during its entire stratigraphic history (until the 1957 earthquake), the resulting age for OSL14 becomes 7.7 ± 0.9 ka, consistent with the radiocarbon ages. This age estimate represents an end-member scenario: complete saturation during the entire history of the sample. Because the luminescence ages from the other sites and the radiocarbon ages from site 5 yield generally consistent results, we believe that the OSL age estimates from site 5 only are erroneously young due to the past influence of groundwater. Therefore, for all three OSL samples from site 5 we report two ages, the first calculated based on current moisture conditions, the second (asterisked and in parentheses) calculated under the assumption of complete saturation until 1957. The true ages of these samples likely lie somewhere in between these estimates based on different groundwater conditions. However, we must make assumptions about sample density and porosity to make the calculations for saturated conditions, and if these assumptions are incorrect, the true age could be outside of the given ranges.

[41] In contrast to sample OSL14, the age estimate of sample OSL13 calculated for unsaturated conditions (5.9 ± 0.7 ka) is consistent with the radiocarbon age of underlying organic horizon D (6.4–6.7 ka; Figure 11), and the age estimate calculated for saturated conditions (8.1 ± 1.3* ka) is too old. Because the measurements of OSL13 were made on feldspar rather than quartz, results from this sample are less reliable, because feldspar is more prone to incomplete bleaching. Because we cannot evaluate the completeness of bleaching for this sample, we do not draw any conclusions from these age estimates. Sample OSL12 (Figure 10) is stratigraphically above unit 6, radiocarbon dated at 5.7–6.0 ka, and both saturated and unsaturated age estimates for this

sample are consistent with available radiocarbon data. The true age of this sample most likely lies somewhere in between the two estimates.

4. Discussion/Conclusions

[42] The most robust and reliable conclusion that we can draw from these data is that the penultimate surface rupture on the Gurvan Bulag fault occurred sometime after 6.0 ka. This conclusion is based on data from site 5, where a unit deformed by the penultimate earthquake (unit 6) has a radiocarbon age of 5.7–6.0 ka. Luminescence ages from units deposited prior to this event at sites 3 and 4 range from 4.1 ± 0.3 ka to 5.8 ± 0.6 ka (Table 5). If both luminescence ages are reliable, the penultimate event occurred sometime after 4.4 ka. This is the maximum age of the youngest preevent sample (OSL6) and therefore the rupture must have occurred after this time.

[43] The luminescence samples from site 5 (OSL12, 13, and 14) also predate the penultimate earthquake. The age estimates for the youngest of these, OSL12, are 2.3 ± 0.2 ka and 3.2 ± 0.4* ka (saturated). If reliable, this suggests the penultimate event occurred after 3.6 ka. However, because of the uncertainty introduced by the problem of groundwater at this site, we prefer the more conservative and more reliable maximum age estimate of sample OSL6 from site 3 to constrain the maximum age (4.4 ka) for the occurrence of the penultimate event.

[44] We have no radiocarbon ages that provide meaningful minimum age constraints on the penultimate event. Therefore, we rely on the OSL ages from sites 3 and 6 (pond and backthrust sites), collected from the colluvial wedges deposited after the penultimate event. These samples give ages of 2.6 ± 0.2 ka (OSL8) and 2.8 ± 0.2 ka (OSL10), consistent with each other and compatible with the maximum age constraint for the penultimate event. If both luminescence ages are reliable, then the minimum age of the older of these (OSL10) provides the minimum age constraint for the penultimate earthquake, 2.6 ka (Table 5). Together with the maximum age constraint, this gives an age range of 2.6–4.4 ka for the occurrence of the penultimate ground rupture on the Gurvan Bulag fault.

[45] The third event back is less well constrained. Some evidence in the site 5 trench suggests that it occurred after the formation of organic horizon E, radiocarbon dated at 7.0–7.3 ka. If we have correlated unit 6 correctly across the trench, then event 3 predates the radiocarbon age of sample RC5, 5.7–6.0 ka. Event 3 also predates the age of luminescence sample OSL3, collected from the colluvial wedge deposited after the prepenultimate event at site 4 (Figure 9). The age estimate of OSL3 is 5.8 ± 0.6 ka, consistent with the radiocarbon age of RC5. Collectively, these results suggest that the third event back occurred sometime in the age range of 5.7–7.3 ka.

[46] These data suggest that three earthquakes (two recurrence intervals) have been associated with rupture of the Gurvan Bulag fault in the last 7.3 ka, and give an average recurrence interval of about 3600 years during this time period. The exposure at site 1 (Western Creek) shows evidence of at least 5 earthquakes since the deposition of the alluvial fan materials (Figure 6). A luminescence date from this terrace surface at site 2 indicates that this alluvial fan was abandoned prior to 26.6 ± 2.1 ka or 16.1 ± 2.0 ka (Table 1). This number of events (five earthquakes, or four recurrence intervals) in this time interval suggests an average recurrence interval of about 6500 years if the 26.6 ka age is correct, or about 4000 years if the 16.1 ka age is correct. A very similar average recurrence interval of 3.3 ± 1 kyr has been derived using estimates of the Gurvan Bulag slip rate (Ritz et al., personal communication).

[47] Our results indicate that the length of earthquake recurrence intervals on the Gurvan Bulag fault is comparable to that on the Bogd fault, i.e., on the order of several thousands of years. However, the little paleoseismic data available for the Bogd fault indicate that the penultimate event on this fault occurred 800–2300 years B.P. (Figure 2) [*Bayasgalan*, 1999] (We have dendrochronologically calibrated the radiocarbon dates reported by *Bayasgalan* [1999].), in contrast to our result of 2600–4400 years B.P. for the Gurvan Bulag fault. Based on the currently available data, the penultimate ruptures of the two faults did not occur during the same earthquake. However, so little paleoseismic data is available for either fault that this conclusion must be considered preliminary, and should be tested with additional study of both faults. Recurrence intervals on both faults are on the order of a few thousand years, and it is therefore likely that the two structures have been intimately related for much of their recent history, and may have ruptured simultaneously in the past. We note that the recurrence interval of the Bogd fault that is inferred from the slip rate estimate, using assumptions of characteristic earthquake magnitude and displacement, is about 3.6 ±1.4 kyr (J. F. Ritz, personal communication, 2002), very similar to our estimates for the Gurvan Bulag. Additional work on both structures, as well as on the other structures that ruptured in 1957, is needed to test this conclusion and to better understand the nature of prehistoric ruptures on this system of faults.

[48] In addition to the information about recurrence of surface ruptures on the Gurvan Bulag fault, our results have another implication regarding the scarps associated with this fault. A vertical component of total slip of at least 5.2 m, based on scarp height, was reported as having formed during the 1957 earthquake [*Kurushin et al.*, 1997]. Near the western end of the Gurvan Bulag rupture, near our sites 1–4, 1957 scarps were reported as up to 3.8 m high [*Kurushin et al.*, 1997]. *Baljinyam et al.* [1993] report a vertical component of total slip of about 3 m calculated from scarp-height measurements in the area about 0.5 km east of our site 4 (P. Molnar, personal communication, 1997). However, stratigraphic relations in our excavations show that the 2- to 4-m-high scarps we studied were built as a consequence of multiple earthquake ruptures, and did not form entirely in 1957. There is no significant difference between the scarp height at our sites 1–4 and the region where *Baljinyam et al.* [1993] made their measurements. In addition, our data from sites 1, 2 and 3 indicate that the 1957 fault slip was approximately 2.1, 2.9 and 2.4 meters, respectively. Although these are minimum fault slip estimates, it seems unlikely that the true values are significantly larger. A 2.9-meter fault displacement would result in a vertical component of displacement of about 1–2 m on faults with the dips observed in our excavations (V = SsinA where V = vertical component of displacement, S = fault slip, and A = fault dip angle. We used fault dip angles of 53° (site 2), and 55° and 18° (site 3) in this calculation). Thus

we suspect that the 1957 scarp heights reported by earlier workers may not have been the result of only the 1957 earthquake, but may be the products of repeated fault ruptures. A similar conclusion was reached by *Carretier et al.* [2002]. Strong ground motion and rupture of multiple fault strands along the Guvan Bulag in 1957 may have freshened preexisting scarps in addition to creating new ruptures. The result may have been the appearance of a fresh rupture for the whole scarp. This situation provides an important cautionary note for future studies of reverse-fault ruptures. An apparently fresh scarp that seems to have formed in a single event may, in fact, be the product of multiple earthquakes. It may be difficult to make meaningful postearthquake measurements of scarp height in environments similar to that of the Gurvan Bulag. To obtain reliable information on coseismic rupture characteristics, it is necessary to have information about preearthquake scarp heights, or to have trench exposures that reveal the geometry of the near-surface fault planes, the amount of fault slip, and the number of events recorded in the near-surface stratigraphy.

[49] Little is known about the repetition of earthquakes that produce rupture on multiple faults, because few paleoseismic studies have been made in these settings. Ruptures such as the 1957 Gobi Altay earthquake stand in contrast to some other historical fault ruptures, such as the 1906 and 1857 earthquakes on the San Andreas fault in California, both of which were associated with significant rupture on only the San Andreas fault [*Lawson*, 1908]. Whether earthquakes that rupture multiple faults repeat this behavior while earthquakes that rupture a single fault zone are repeatedly confined to a single fault is an important question in understanding seismic hazard. *Bayarsayhan et al.* [1996] suggest that the complexity of the 1957 Gobi Altay earthquake may be analogous to a potential future earthquake in southern California. They postulate that a future earthquake could simultaneously rupture the San Andreas fault along with the Sierra Madre and other nearby faults, producing a similar rupture pattern to that of the 1957 Gobi Altay earthquake. However, the most recent rupture of the San Andreas fault in southern California, the 1857 Fort Tejon earthquake, produced significant rupture only on the San Andreas fault. Furthermore, paleoseismic data from the Sierra Madre fault suggest that the most recent earthquake to cause surface rupture of this fault occurred more than 8 ka [*Tucker and Dolan*, 2001]. These data suggest that an earthquake involving rupture of both the San Andreas and Sierra Madre faults, if possible, must be exceedingly rare. Further testing of the *Bayarsayhan et al.* [1996] hypothesis requires additional knowledge of the past behavior of the southern California structures involved in addition to a general understanding of the past behavior of multiple-fault ruptures worldwide.

[50] Although a number of large, twentieth century earthquakes produced rupture on multiple faults, paleoseismic studies on multiple-rupture events have been conducted only on the M7.3 1992 Landers [*Sieh et al.*, 1993] and the M7.1 1999 Hector Mine [*Treiman et al.*, 2002] earthquakes in southern California. The Landers earthquake involved slip on five distinct strike-slip faults, with no or only minimal components of normal or reverse faulting [*Sieh et al.*, 1993]. Paleoseismic data available for the Landers ruptures suggests that the penultimate rupture may also have involved some, but did not involve all, of the same faults as the 1992 event [*Rockwell et al.*, 2000; *Rubin and Sieh*, 1997]. The 1999 Hector Mine earthquake involved slip on two distinct strike-slip faults [*Treiman et al.*, 2002]. Paleoseismic studies on these faults have not determined whether they may have ruptured together in the past [*Rymer et al.*, in press; *Lindvall et al.*, 2001]. Our results suggest that although their repeat times are similar, the Gurvan Bulag and Bogd faults do not always rupture together as they did in 1957, leaving open the possibility that earthquakes in this region might not always involve slip on multiple faults. Additional paleoseismic study is needed on all the structures involved in the 1957 rupture, as well as nearby Quaternary faults that did not rupture in 1957, to answer the question of whether the Bogd fault sometimes ruptures alone. Paleoseismic study of other historical multiple-fault surface ruptures is needed to determine whether or not multiple-fault and single-fault ruptures tend to repeat in a self-similar fashion.

[51] **Acknowledgments.** Many thanks for field support to: Altaa, Bataa, Chinbat, Erdene, Ganbold, Orgil and Tumee, for driving, vehicle repair, trench digging, cooking and frisbee games. We wish to thank M. Ganzorig of the Informatics and Remote Sensing Center, Ulaanbaatar, Mongolia, for logistical support. Support for this project was provided by the Nuclear Regulatory Commission, through funding to David Schwartz at the USGS. We are grateful to Shannon Mahan, who provided measurements of radionuclide concentrations to support the luminescence age estimates, and valuable discussion of those ages. Thanks to Peter Molnar for inspiration and for reviewing the manuscript. Thanks also to reviewer James Dolan, and to Tony Crone, Ken Hudnut and Shannon Mahan for very helpful reviews of an early draft of this manuscript.

References

Adamiec, G., and M. Aitken, Dose-rate conversion factors: Update, *Ancient TL*, *16*(2), 37–50, 1998.

Aitken, M. J., *Thermoluminescence Dating*, 359 pp., Academic, San Diego, Calif., 1985.

Baljinnyam, I., et al., Ruptures of major earthquakes and active deformation in Mongolia and its surroundings, *Geol. Soc. Am. Mem.*, *181*, 62 pp., 1993.

Bayarsayhan, C., A. Bayasgalan, B. Enkhtuvshin, K. W. Hudnut, R. A. Kurushin, P. Molnar, and M. Ölziybat, 1957 Gobi-Altay, Mongolia earthquake as a prototype for southern California's most devastating earthquake, *Geology*, *24*, 579–582, 1996.

Bayasgalan, A., Active tectonics of Mongolia, unpublished Ph.D. dissertation, 182 pp., Trinity Coll., Cambridge Univ., Cambridge, England, 1999.

Berger, G. W., Dating Quaternary events by luminescence, in *Dating Quaternary Sediments*, *Geol. Soc. Am. Spec. Pap. 227*, edited by D. J. Easterbrook, pp. 13–50, 1988.

Berger, G. W., Regression and error analysis for a saturating-exponential-plus-linear model, *Ancient TL*, *8*, 23–25, 1990.

Berger, G. W., Thermoluminescence dating of sediments older than 100 ka, *Quat. Sci. Rev.*, *13*, 445–455, 1994.

Berger, G. W., R. A. Lockhart, and J. Kuo, Regression and error analysis applied to the dose-response curves in thermoluminescence dating, *Nucl. Tracks Radiat. Meas.*, *13*, 177–184, 1987.

Carretier, S., J.-F. Ritz, J. Jackson, and A. Bayasgalan, Morphological dating of cumulative reverse fault scarp: Examples from the Gurvan Bogd fault system, Mongolia, *Geophys. J. Int.*, *148*, 256–277, 2002.

Clarke, M. L., H. M. Rendell, and A. G. Wintle, Quality assurance in luminescence dating, *Geomorphology*, *29*, 173–185, 1999.

Florensov, N. A., and V. P. Solonenko (Eds.), *The Gobi-Altay Earthquake*, 424 pp., U.S. Dep. of Commer., Washington, D. C., 1965.

Huntley, D. J., and A. G. Wintle, The use of alpha scintillation counting for measuring Th-230 and Pa-231 contents of ocean sediments, *Can. J. Earth Sci.*, *18*, 419–432, 1981.

Kurushin, R. A., A. Bayasgalan, M. Ölziybat, B. Enkhtuvshin, P. Molnar, C. Bayarsayhan, K. W. Hudnut, and J. Lin, The surface rupture of the 1957 Gobi-Altay, Mongolia, earthquake, *Geol. Soc. Am. Spec. Pap.*, *320*, 143 pp., 1997.

Lawson, A. C., *The California earthquake of April 18, 1906, Report of the State Earthquake Investigation Commission*, *Publ. 87*, Carnegie Institute of Washington, 451 pp., Washington, D. C., 1908.

Lindvall, S., et al., 1999 M7.1 Hector Mine earthquake surface rupture and adjacent Bullion fault, Twentynine Palms Marine Corps Base, California (abstract), *Geol. Soc. Am. Abstr. Programs*, *33*, 79, 2001.

McCalpin, J. P., (Ed.), *Paleoseismology*, 588 pp., Academic, San Diego, Calif., 1996.

Ollerhead, J., D. J. Huntley, and G. W. Berger, Luminescence dating of the Buctouche Spit, New Brunswick, *Can. J. Earth Sci.*, *31*, 523–531, 1994.

Prescott, J. R., and J. T. Hutton, Cosmic ray and gamma ray dosimetry for TL and ESR, *Nucl. Tracks Radiat. Meas.*, *14*, 223–227, 1988.

Ritz, J. F., E. T. Brown, D. L. Boulés, H. Philip, A. Schlupp, G. M. Raisbeck, F. Yiou, and B. Enkhtuvshin, Slip rates along active faults estimated with cosmic-ray-exposure dates: Application to the Bogd fault, Gobi-Altaï, Mongolia, *Geology*, *23*, 1019–1022, 1995.

Ritz, J. F., et al., Analysing variations of uplift rates along the Gurvan Bulag thrust fault (Gobi-Altay, Mongolia), during the Upper Pleistocene. Consequences in terms of seismic activity (abstract), *EOS Trans. AGU*, *80*, 1039, 1999.

Ritz, J.-F., et al., Late Pleistocene to Holocene slip rates for the Gurvan Bulag thrust fault (Gobi-Altay, Mongolia) estimated with 10Be dates, *J. Geophys. Res.*, doi:10.1029/2001JB000553, in press, 2002.

Rockwell, T. K., S. Lindvall, M. Herzberg, D. Murbach, T. Dawson, and G. Berger, Paleoseismology of the Johnson Valley, Kickapoo, and Homestead Valley faults of the Eastern California Shear Zone, *Bull. Seismol. Soc. Am.*, *90*, 1200–1236, 2000.

Rubin, C. M., and K. Sieh, Long Dormancy, Low Slip Rate and Similar Slip-per-Event for the Emerson fault, Eastern California Shear Zone, *J. Geophys. Res.*, *102*, 15,319–15,330, 1997.

Rymer, M. J., G. G. Seitz, K. D. Weaver, A. Orgil, G. Faneros, J. C. Hamilton, and C. Goetz, Geologic and paleoseismic study of the Lavic Lake fault at Lavic Lake playa, Mojave Desert, southern California, *Bull. Seismol. Soc. Am.*, *92*, in press.

Sieh, K. E., et al., Near-field investigations of the Landers earthquake sequence, April to July 1992, *Science*, *260*, 171–176, 1993.

Stuiver, M., and P. J. Reimer, Extended ^{14}C data base and revised CALIB 3.0 ^{14}C age calibration program, *Radiocarbon*, *35*, 215–230, 1993.

Stuiver, M., P. J. Reimer, E. Bard, J. W. Beck, G. S. Burr, K. A. Hughen, B. Kromer, F. G. McCormac, J. v. d. Plicht, and M. Spurk, INTCAL98 radiocarbon age calibration, 24,000-cal BP, *Radiocarbon*, *40*, 1041–1083, 1998.

Treiman, J. A., K. J. Kendrick, W. A. Bryant, T. K. Rockwell, and S. F. McGill, Primary surface rupture associated with the Mw7.1 16 October, 1999 Hector Mine earthquake, San Bernardino County, California, *Bull. Seismol. Soc. Am.*, *92*, 1171–1191, 2002.

Tucker, A. Z., and J. F. Dolan, Paleoseismologic evidence for a >8 ka age for the most recent surface rupture on the eastern Sierra Madre fault, northern Los Angeles metropolitan region, *Bull. Seismol. Soc. Am.*, *91*, 232–249, 2001.

Yeats, R. S., K. Sieh, and C. R. Allen, *The Geology of Earthquakes*, 568 pp., Oxford Univ. Press, New York, 1997.

A. Bayasgalan, GeoInformatics Research and Training Center, Mongolian University of Science and Technology (MUST), P.O. Box 49/418, Ulaanbaatar, Mongolia.

K. Berryman, Institute of Geological and Nuclear Sciences Ltd., 69 Gracefield Road, P.O. Box 30-368, Lower Hutt, New Zealand.

K. Kendrick, U.S. Geological Survey, 525 South Wilson Street, Pasadena, CA 91106, USA.

C. S. Prentice, U.S. Geological Survey, 345 Middlefield Road, Menlo Park, CA 94025, USA. (cprentice@isdmnl.wr.usgs.gov)

J. F. Ritz, Institut des Sciences de la Terre, de l'Eau et de l'Espace de Montpellier, Universite Montpellier II, Place Eugene Bataillon, 34095 Montpellier Cedex 05, France.

J. Q. Spencer, School of Geography and Geosciences, University of St. Andrews, St. Andrews Fife, KY16 9AL, Scotland, UK.